Hindawi Publishing Corporation
Journal of Spectroscopy
Volume 2014, Article ID 619373, 8 pages
http://dx.doi.org/10.1155/2014/619373

Research Article

Interaction of Bradykinin and B_2 Bradykinin Receptor Antagonists with Colloidal Au Surface Explored by Surface-Enhanced Raman Scattering

Dominika Skołuba,[1] Dariusz Sobolewski,[2] Adam Prahl,[2] and Edyta Proniewicz[3]

[1] *Faculty of Chemistry, Jagiellonian University, Ulica Ingardena 3, 30-060 Krakow, Poland*
[2] *Department of Chemistry, University of Gdansk, Sobieskiego 18, 80-592 Gdansk, Poland*
[3] *Faculty of Foundry Engineering, AGH University of Science and Technology, ul. Reymonta 23, 30-059 Krakow, Poland*

Correspondence should be addressed to Edyta Proniewicz; proniewi@agh.edu.pl

Received 2 September 2013; Accepted 12 October 2013; Published 4 February 2014

Academic Editor: Yizhuang Xu

Bradykinin (BK), an endogenous peptide hormone, which is involved in a number of physiological and pathophysiological processes, and the potent B_2 bradykinin receptor antagonists, [D-Arg^0,Hyp^3,Thi^{5,8},L-Pip^7]BK, Aaa[D-Arg^0,Hyp^3,Thi^{5,8},L-Pip^7]BK, [D-Arg^0,Hyp^3,Thi^5,D-Phe^7,L-Pip^8]BK, and Aaa[D-Arg^0,Hyp^3,Thi^5,D-Phe^7,L-Pip^8]BK, were deposited onto colloidal Au particles of 20 nm size. Interaction of these molecules with colloidal Au surface was explored by surface-enhanced Raman scattering (SERS). Briefly, it was shown that BK adsorbs on the Au surface mainly through the Phe^5/Phe^8 residues. In case of the BK specifically modified analogues mainly the Pip and Thi rings are involved in the interaction process; however, Pip and Thi adopt slightly different orientation with respect to Au for each of the analogues. In addition, the lack of the Aaa vibrations, together with the enhancement of the Thi, Pip, or Phe modes, emphasizes the importance of the *C*-terminus in the interaction with the Au surface.

1. Introduction

Bradykinin (BK; Arg^1-Pro^2-Pro^3-Gly^4-Phe^5-Ser^6-Pro^7-Phe^8-Arg^9) is an important endogenous oligopeptide counted from the family of kinins [1]. Biological activities of BK are associated with a number of physiological and pathophysiological processes, including regulation of vascular permeability, formation of edema, stimulation of nerve endings, and inflammation process [2, 3]. It is also a potent cancers growth factor, especially prostate and lung carcinoma [4, 5]. Biological effects of BK are mediated by activation of the G protein coupled seven transmembrane receptors (GPCRs), named B_1 and B_2 [6]. GPCRs are the largest group of the membrane receptors [7]. The B_1 receptors are poorly detectable under physiological conditions, whereas the B_2 receptors are continuously produced. The B_2 receptors mediate most of the biological effects and demonstrate a high affinity for BK [8].

The biological significance of BK motivated researchers to explore behavior of this peptide at different solid/liquid interfaces. For example, studies using nuclear magnetic resonance (NMR) [9, 10], circular dichroism (CD) [11], and molecular dynamics [12] have explored mode of BK binding to different membranes and pointed out the formation of the BK *C*-terminal (Ser^6-Arg^9) β-turn structure in the membrane-bound state of BK that is crucial for this binding to the B_2 receptor [12, 13]. Studies on BK adsorbed onto the electrochemically roughened Ag, Au, and Cu electrode surfaces in an aqueous solution at physiological pH at different applied electrode potential have shown that BK interacts mainly through the two Phe (L-phenylalanine), Arg (L-arginine), and Pro (L-proline) residues, but in different arrangements, with each of the metal surfaces [14]. These results are similar to those from the biological activity studies [15]. Also, experiments for isotopically labeled BK deposited onto the Ag electrode have demonstrated that the reorientation

of the BK phenyl rings cannot keep up with the electrode potential changes at the electrode potential range from −0.8 to −0.4 V [16]. Another examination of four of the B_2 BK receptor antagonists immobilized onto Ag SERS-active: ROC (prepared in the reduction-oxidation cycles) and colloidal substrates have demonstrated that the adsorption mode of BK varied in time on the ROC substrate and the ROC surface is more selective than the colloidal one [17, 18].

In this work, using surface-enhanced Raman spectroscopy (SERS) we characterized adsorption mode of BK and its four synthetic B_2 BK receptor antagonists: [D-Arg^0,Hyp^3,Thi^{5,8},L-Pip^7]BK, Aaa[D-Arg^0,Hyp^3,Thi^{5,8},L-Pip^7]BK, [D-Arg^0,Hyp^3,Thi^5,D-Phe^7,L-Pip^8]BK, and Aaa[D-Arg^0,Hyp^3,Thi^5,D-Phe^7,L-Pip^8]BK (where Aaa denotes 1-adamantaneacetic acid, Hyp—L-hydroxyproline, Thi—L-thienylalanine, and Pip—L-pipecolic acid) onto colloidal Au spheres with the diameters of approximately 20 nm. The SERS technique was earlier used in our laboratory to correlate the structural components of the many different peptides, including bombesin, vasopressin, neurotensin, and their modified analogs with their capability to interact with the proper metabotropic receptor [19–22]. Also, our aim is correlation of information resulting from the spectroscopic and biological activity investigations.

Since 1979, it is known that the composition of the metallic nanostructures has influence on the intensity of the SERS signal. Ag enhances the Raman signal more (10–100-fold) than Au because of the plasmon resonance [23]. In addition, Ag can be excited in the light range from the UV to the IR, whereas Au is limited to the red or IR due to damping by the interband transitions [24]. Despite these limitations, essential structural studies for living organisms are commonly performed for Au. It is due to significantly higher biocompatibility and better control of the size and shape of Au in comparison to the Ag nanostructures [25].

2. Materials and Methods

2.1. Peptide Synthesis. BK, [D-Arg^0,Hyp^3,Thi^{5,8},L-Pip^7]BK, Aaa[D-Arg^0,Hyp^3,Thi^{5,8},L-Pip^7]BK, [D-Arg^0,Hyp^3,Thi^5,D-Phe^7,L-Pip^8]BK, and Aaa[D-Arg^0,Hyp^3,Thi^5,D-Phe^7,L-Pip^8]BK were obtained by the solid-phase method using the Fmoc-strategy starting from Fmoc-Arg(Pbf)-Wang resin (GL Biochem Shanghai Ltd., 1% DVB, 100–200 mesh, 0.47 mmol/g) [26]. Fmoc was removed by 20% piperidine in DMF. A 3-fold excess of the respective Fmoc-amino acids was activated *in situ* using HATU (1 eq)/HOAt (1 eq) in a mixture of DMF/NMP (1 : 1 v/v) containing 1% Triton, and the coupling reactions were base-catalyzed with NMM (2 eq). The amino acid side-chain-protecting groups were Bu^t for Hyp and Ser and Pbf for Arg and D-Arg. All of the Fmoc-protected amino acids were commercially available (NovaBiochem, Bad Soden, Germany). Aaa (1-adamantaneacetic acid) was coupled in the final coupling step (for acylated peptides) using the same procedure as that for Fmoc-amino acids. Cleavage of the peptides from the resin with side-chain deprotection was performed by treatment with TFA : H_2O : TIS (95 : 2.5 : 2.5 v/v/v) for 4 h. The total volume of the TFA filtrate was reduced to approximately 1 mL by evaporation *in vacuo*. The peptides were precipitated with cold diethyl ether and filtered through a Schott funnel. All of the peptides were purified by semipreparative high-performance liquid chromatography (HPLC). HPLC was executed on a Waters (analytical and semipreparative) chromatograph equipped with a UV detector (λ = 226 nm). The purity of the peptides was determined on a Discovery HS C_{18} column (5 μm, 100 Å; 250 × 4.6 mm). The solvent systems were (A) 0.1% aqueous trifluoroacetic acid (TFA) and (B) 80% acetonitrile in aqueous 0.1% TFA (v/v). A linear gradient from 1 to 80% of (B) over 30 min was applied for peptides at a flow rate of 1 mL/min. Semipreparative HPLC was performed using a Kromasil C_8 column (5 μm, 100 Å; 16 × 250 mm) in a linear gradient from 10 to 40% of (B) for 90 min at a flow rate of 8 mL/min. The mass spectra of the peptides were recorded on a Bruker BIFLEX III MALDI TOF mass spectrometer (ionization: 337 nm nitrogen laser).

2.2. SERS Measurement in Au Colloid Solution. The Au colloid was purchased from Sigma Aldrich (stabilized suspension in citrate buffer, diameter 20 nm). Aqueous solution of the peptides was prepared by dissolution of the peptides in deionized water. The concentration of the peptide solutions was adjusted to 10^{-4} M before them being mixed with the Au colloid. 10 μL of peptide sample was mixed with 20 μL of Au nanoparticles. The SERS spectra of the peptides were obtained using Renishaw spectrometer (model inVia) operating in confocal mode combined with a Peltier cooled CCD detector and a Leica microscope (50x long-distance objective). Excitation wavelength at 785 nm was used from HP NIR diode laser. The laser power at the laser output was set at approximately 20 mW. Generally, the SERS spectra were measured at four spots on the surfaces of the colloidal Au nanoparticles and were obtained during 2 h of sample addition to the Au solution. The spectra from the series were nearby identical, except for small differences in some band intensities. During measurements no spectral changes due to the sample decomposition or desorption processes were observed.

2.3. Spectral Analysis. The spectral analysis was performed using the GRAMS/AI 8.0 (Thermo Electron Corp.).

3. Results and Discussion

Figure 1 presents the SERS spectra of Figure 1(a) BK and its four potent B_2 BK receptor antagonists: Figure 1(b) [D-Arg^0,Hyp^3,Thi^{5,8},L-Pip^7]BK, Figure 1(c) Aaa[D-Arg^0, Hyp^3,Thi^{5,8},L-Pip^7]BK, Figure 1(d) [D-Arg^0, Hyp^3,Thi^5,D-Phe^7,L-Pip^8]BK, and Figure 1(e) Aaa[D-Arg^0,Hyp^3,Thi^5,D-Phe^7,L-Pip^8]BK (see Table 1 for molecular structures) in the Au aqueous solution excited with 785 nm line. The spectral positions of the enhanced bands in these spectra, given in wavenumbers, are summarized in Table 2 together with the proposed vibrational assignments. This assignment leans on the earlier studies of amino acids lyophilized and deposited

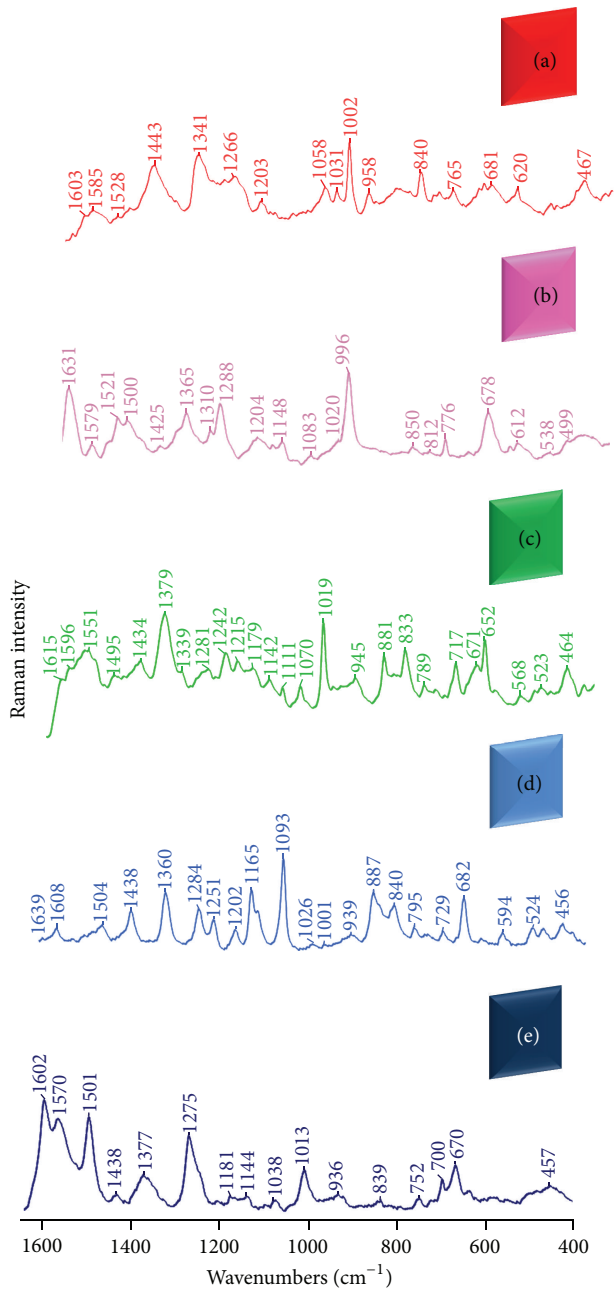

FIGURE 1: The SERS spectra of (a) BK and its analogues: (b) [D-Arg^0,Hyp^3,Thi^{5,8},L-Pip^7] BK, (c) Aaa[D-Arg^0,Hyp^3,Thi^{5,8},L-Pip^7]BK, (d) [D-Arg^0,Hyp^3,Thi^5,D-Phe^7,L-Pip^8]BK, and (e) Aaa[D-Arg^0,Hyp^3,Thi^5,D-Phe^7,L-Pip^8]BK adsorbed onto a colloidal Au particles surface in an aqueous solution.

onto the colloidal Au surface [27, 28], BK, and its modified analogs [16–18], piperidine (Pip) [29, 30] and thiophene (Thi) [31–33]. Based on the analysis of the changes in the bands enhancement, bands width, and shift in bands wavenumber between corresponding Raman [14, 16–18] and SERS spectra conclusions about the adsorption process of BK and its four analogs deposited onto the colloidal Au surface were drawn as described below.

The SERS spectrum of BK (Figure 1(a)) is dominated by 1603 [ν_{8a}], 1585 [ν_{8b}], 1443 [ν_{19b}], 1203 [ν_{7a}], 1031 [ν_{18a}], 1002 [ν_{12}], and 620 cm^{-1} [ν_{6b}] bands due to the Phe residues (Phe^5/Phe^8) vibrations. According to the so-called surface selection rules, the phenyl ring orientation with respect to the colloidal Au substrate could be predicted based on the relative intensity of the aforementioned bands [34, 35]. For a perpendicular orientation of an aromatic ring onto metal surface these rules postulate that the in-plane modes should be mainly enhanced in the SERS spectra. On the other hand, for a horizontal orientation of the aromatic ring on the metal surface the out-of-plane vibrations should be stronger than

Table 1: Amino acid sequence of bradykinin (BK) and its specifically mutated analogues investigated in this work.

Analogue	Amino acid sequence										
	0′	0	1[a]	2[a]	3	4[a]	5	6[a]	7	8	9[a]
BK			Arg	Pro	Pro	Gly	Phe	Ser	Pro	Phe	Arg
[D-Arg^0,Hyp^3,Thi^{5,8},L-Pip^7]BK		D-Arg	Arg	Pro	Hyp	Gly	Thi	Ser	L-Pip	Thi	Arg
Aaa[D-Arg^0,Hyp^3,Thi^{5,8},L-Pip^7]BK	Aaa	D-Arg	Arg	Pro	Hyp	Gly	Thi	Ser	L-Pip	Thi	Arg
[D-Arg^0,Hyp^3,Thi^5,D-Phe^7,L-Pip^8]BK		D-Arg	Arg	Pro	Hyp	Gly	Thi	Ser	D-Phe	L-Pip	Arg
Aaa[D-Arg^0,Hyp^3,Thi^5,D-Phe^7,L-Pip^8]BK	Aaa	D-Arg	Arg	Pro	Hyp	Gly	Thi	Ser	D-Phe	L-Pip	Arg

Aaa: 1-adamantaneacetic acid Hyp: L-hydroxyproline Thi: L-thienylalanine Pip: L-pipecolic acid

[a]Common amino acid in the sequence of all investigated analogues.

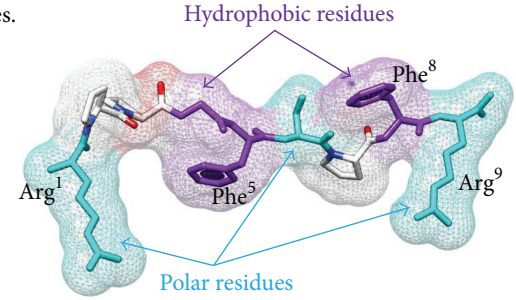

the in-plane vibrations. Thus, based on the propensity rules and phenomenon that the in-plane 1002 cm^{-1} band is the strongest band in the BK SERS spectrum and is less intense than that in the BK Raman spectrum it can be suggested that the BK phenyl rings adopt the tilted orientation with respect to the Au nanoparticles surface [14, 16]. The neglected shift in wavenumber and 4 cm^{-1} band broadening of the 1002 cm^{-1} SERS signal in comparison with those in the corresponding Raman spectrum together with the symmetric shape of this band indicate that the BK phenyls rings do not interact directly with Au. Thus, should be located in slight distance from Au.

Apart from the phenyl rings, the Arg and Pro residues are also involved in the interaction of BK with the colloidal Au surface. The Arg and Pro oscillations at 1443 [δ(NH)], 1341 [ρ_{sb} (CH_3)], 1058 [ν(CC) + ν(NC)], and 840 [δ(NH)] cm^{-1} and at 1528, 1443, and 765 cm^{-1} (see Table 2 for the bands assignment), respectively, determine this interaction.

In the SERS spectrum of [D-Arg^0,Hyp^3,Thi^{5,8},L-Pip^7]BK (Figure 1(b)) the weak 1579, 1310, 1148, 1020, 850, 776, 612, and 499 cm^{-1} and the strong 1288 and 996 cm^{-1} spectral features (see Table 2 for bands assignment) point out the interaction between Pip^7 and the colloidal Au surface. The broadness and pronounced intensity of the last two SERS bands additionally suggest the participation of the free electron-pair on the Pip^7 nitrogen atom in this interaction. This is possible when the Pip^7 ring adopts the tilted orientation. Also, Thi and Arg contribute to the SERS spectrum of [D-Arg^0,Hyp^3,Thi^{5,8},L-Pip^7]BK onto the Au surface. This conclusion is based on the appearance of the 1521, 1500[δ(CH)+ν(C=C), in-plane], 1365 [(δ(CH)+ν(C=C), in-plane], 1083 [ρ_r(CH), in-plane], 850 [δ(ring) + $\nu(CC)_{ring}$, in-plane], and 678 cm^{-1}[(ν(CH), out-of-plane] bands due to Thi [31, 32]. The similar medium relative enhancement of the in-plane and out-of-plane Thi modes implies the tilted orientation of the Thi ring with respect to the Au nanoparticles surface. On the other hand, the interaction of the guanidine group with colloidal Au surface is manifested by the 1631, 1425, and 1365 cm^{-1} SERS signals.

Addition of Aaa at the *N*-terminal end of [D-Arg^0,Hyp^3,Thi^{5,8},L-Pip^7]BK produces marked changes in the SERS spectral pattern as is evident in Figure 1(c) (the Aaa[D-Arg^0,Hyp^3,Thi^{5,8},L-Pip^7]BK analog). In the spectrum of Aaa[D-Arg^0,Hyp^3,Thi^{5,8},L-Pip^7]BK in the Au solution, the 1596, 1551, 1379, 1281, 1242, 1179, 1142, 1019, 881, 833, 652, and 464 cm^{-1} (see Table 2 for bands assignment) signals are due to Pip^7. Among these, the 1379 and 1019 cm^{-1} bands exhibit the predominant relative intensity (Figure 1(c)) what point out on the vertical orientation of Pip^7 on the Au surface. Although it seems that the Pip^7 nitrogen atom does not participate directly with this surface (weak 1281 cm^{-1} band). Also, bands due to the Thi vibrations (1495, 1215, 1179, 1070, 881, 833, 671, and 568 cm^{-1}) are weakly enhanced in the Aaa[D-Arg^0,Hyp^3,Thi^{5,8},L-Pip^7]BK SERS spectrum. This is why we suggest that Thi assists in the adsorption process onto the Au surface.

In the SERS spectrum of [D-Arg^0,Hyp^3,Thi^5,D-Phe^7,L-Pip^8]BK (Figure 1(d)), the phenyl ring (D-Phe^7) modes (1608, 1026, and 1001 cm^{-1}) are weakly enhanced. Unlike those, the

Table 2: Wavenumbers and proposed band assignments for SERS spectra of A: BK, B: [D-Arg^0,Hyp^3,Thi^{5,8},L-Pip^7]BK, C: Aaa[D-Arg^0,Hyp^3,Thi^{5,8},L-Pip^7]BK, D: [D-Arg^0,Hyp^3,Thi^5,D-Phe^7,L-Pip^8]BK, and E: Aaa[D-Arg^0,Hyp^3,Thi^5,D-Phe^7,L-Pip^8]BK adsorbed onto colloidal gold surface.

	Wavenumber/cm^{-1}				
	A	B	C	D	E
$\rho_s(NH_2)$, Arg[ν_s(C=N)], and/or Amide I	—	1631	1615	1639	—
Phe[ν_{8a}] and/or Arg[$\delta(NH_2^+)$ + ν_s(C=N)]	1603	—	—	1608	1602
Phe[ν_{8b}] and/or Pip and/or Arg[δ(NH)]	1585	1579	1596	—	1570
Pip	—	—	1551	—	—
Imide II' and/or Thi[ν(CC)]	1528	1521	—	—	—
Thi[ν(C–C)]	—	1500	1495	1504	1501
Phe[ν_{19b}], Arg[δ(NH)], and/or tertiary amide IIp marker	1443	1425	1434	1438	1438
Thi[δ(CH) + ν(C=C)], Pip combination, and/or $\nu(COO^-)$	—	1365	1379	1360	1377
Arg[$\rho_{sb}(CH_3)$]	1341	—	1339	—	—
Pip[$\rho_w(CH_2)$]	—	1310	—	—	—
Pip[ν(CN) + ρ_b(CCH) + $\rho_{r/t}(CH_2)$] and/or Amide III	—	1288	1281	1284	1275
Phe[ν_4]	1266	—	—	—	—
Pip[$\rho_t(CH_2)$] and/or Amide III	—	—	1242	1251	—
Phe[ν_{7a}]	1203	—	—	—	—
Thi[ν(CH)]	—	1204	1215	1202	1212
Arg[ν(CN)] and/or Thi[ρ_r(CH)]	—	1170	1179	1165	1181
Arg[ν(CCC)] and/or Pip[$\rho_t(CH_2)$]	—	1148	1142	1151	1144
Aaa[ν(CC)]	—	—	1111	—	1102
Thi[in-plane ρ_r(CH)] and/or Arg [ν(CN)]	—	—	—	1093	—
Arg[ν(CN)] and/or Thi[ρ_r(CH)]	—	1083	1070	—	1083
Arg[ν(CC) + ν(NC)]	1058	—	—		1045
Phe[ν_{18a}]	1031	—	—	1026	
Pip[skeletal stretching]	—	1020 996	1019		1013
Phe[ν_{12}]	1002	—	—	1000	—
ν(CC) + $\rho_r(CH_2)$	958	—	945	957	—
	—	—	—	939	936
Arg[$\rho_b(NH_2)$], Pip[ρ_r(CH)], and/or Thi[$\rho_w(CH_2)$ + γ(ring)]	—	—	—		925
Thi[δ(ring) + ν(CS)] and/or Pip skeletal stretching	—	—	881	887	—
Arg[δ(NH)], Thi[δ(ring) + ν(CC)], and/or Pip ν(CC)	840	850	—	840	—
Pip ring breathing, Arg[$\rho_w(NH_2)$], and/or Thi[ν(CC) + δ(ring)]	—	812	833		839
Pip[ring breathing]	—	776	763	763	752
Pro[$\rho_r(CH_2)_{ring}$]	765	—	—		—
Pip	—	723	—	729	725
Pip	—	—	717		700
Thi[ρ_w(CH)] and/or Arg [$\delta(COO^-)$]	681	678	671	682	670
ρ_b(COO) and/or Amide	—	—	652	—	—
Phe[ν_{6b}]	620	—	—	—	—
Pip	—	612	—	594	—
Thi[γ(ring) + $\rho_w(CH_2)$]	—	—	568	—	—
ρ_b(CO) and/or $\rho_r(CH_2)$	—	538	—	534	—
Pip	—	499	—	—	—
Skeletal	467	—	464	—	457
Thi[γ(ring)]	—	—	426	—	—

ν: stretching, δ: deformation, γ: torsion, ρ_t: twisting, ρ_b: bending ρ_r: rocking, ρ_w: wagging, and ρ_s: scissoring vibrations; Phe: phenylalanine, Arg: arginine, Thi: L-thienylalanine, Aaa: 1-adamantaneacetic acid, and Pip: L-pipecolic acid.

bands mainly connected with the Thi^5 ring dominate this spectrum (at 1504, 1360, 1165, 1093, 887, 840, and 682 cm^{-1}). These results are in contrast to those obtained for the abovementioned analog adsorbed on the colloidal Ag surface [18] and suggest that the D-Phe^7 ring is removed from the Au surface (no shift in the Phe bands wavenumber and width), whereas the Thi^5 adopts the vertical arrangement on this surface. The appearance bands at 1284, 1251, 1151, 887, 840, 763, 729, and 594 cm^{-1} indicate that also Pip^8 contributed to the SERS spectrum on Au surface. Of these bands, 1284 and 1151 cm^{-1} SERS signals (mainly enhanced) are due to the in-plane Pip^8 ring vibrations. For this reason we imply that Pip^8 assists in adsorption process and is oriented vertically on this substrate through the lone electron pair of the nitrogen atom. The Arg$\cdots$Au interactions cannot be excluded for this peptide because of the 1639, 1608, 1438, 1165, 939, and 840 cm^{-1} spectral features. Based on these observations mainly the guanidine group appear to be in proximity to the Au surface (Table 2).

In the case of Aaa[D-Arg^0,Hyp^3,Thi^5,D-Phe^7,L-Pip^8]BK SERS spectrum (Figure 1(e)), both the Pip^8 and Thi^5 rings modes are enhanced. Pip^8 gives rise to the 1570, 1275, 1181, 1144, 1013, 839, and 752 cm^{-1} spectral features, whereas the 1501 (the most intense, in-plane mode), 1377, 1144, and 670 cm^{-1} SERS signals are related to the Thi^5 vibrations. Analysis of the Pip^8 bands' relative intensity, bands width, and bands wavenumber changes suggested that, similarly as in the case of [D-Arg^0,Hyp^3,Thi^{5,8},L-Pip^7]BK, Pip^8 in Aaa[D-Arg^0,Hyp^3,Thi^5,D-Phe^7,L-Pip^8]BK being tilted with respect to the colloidal Au surface interacts with this surface through the nitrogen-free electrons pair. However, it seems that the strength of this interaction is higher for Aaa[D-Arg^0,Hyp^3,Thi^5,D-Phe^7,L-Pip^8]BK than for [D-Arg^0,Hyp^3,Thi^{5,8},L-Pip^7]BK. Much of the same analysis for the Thi^5 bands implies that the Thi^5 ring assists in the adsorption process adopting the near-edge-on orientation onto the colloidal Au surface. What is interesting in case of the Aaa[D-Arg^0,Hyp^3,Thi^5,D-Phe^7,L-Pip^8]BK SERS spectrum (Figure 1(e)) is that we observed apart from bands at 1438, 1083, 936, 839, and 670 cm^{-1} very significantly enhanced overlapped, broad bands at 1602 [$(\delta(NH_2^+) + \nu_s(C{=}N)$] and 1570 [$\delta$(NH]. Based on these observations we suggest that we above all observed interaction between Arg's –NH_2-group from the guanidine group and Au surface.

4. Conclusions

In this study, we reported the mode of adsorption of BK and its potent B_2 receptor antagonists: [D-Arg^0,Hyp^3, Thi^{5,8},L-Pip^7]BK, Aaa[D-Arg^0,Hyp^3,Thi^{5,8},L-Pip^7]BK, [D-Arg^0,Hyp^3, Thi^5,D-Phe^7,L-Pip^8]BK, and Aaa[D-Arg^0,Hyp^3,Thi^5,D-Phe^7, L-Pip^8]BK adsorbed on the colloidal Au surface. We showed the following.

(i) The Phe^5/Phe^8 residues (in tilted orientation of the rings) are mainly involved in the BK interaction with the colloidal Au surface, whereas D-Phe^7 in [D-Arg^0,Hyp^3,Thi^5,D-Phe^7,L-Pip^8]BK and Aaa[D-Arg^0,Hyp^3,Thi^5,D-Phe^7,L-Pip^8]BK is moved out of this surface; thus it is located on the opposite side of the polypeptide backbone.

(ii) Pip and Thi adsorb on the colloidal Au surface for all the investigated BK analogues. The Thi and Pip residues in [D-Arg^0,Hyp^3,Thi^{5,8},L-Pip^7]BK adsorb in the tilted orientation on the Au surface (Pip through the piperidine nitrogen atom). Elongation of the peptide backbone by the addition of Aaa at the *N*-termini (the Aaa[D-Arg^0,Hyp^3,Thi^{5,8},L-Pip^7]BK analog) produces rearrangement of the Pip ring (it rises and there is no longer interaction between the piperidine nitrogen atom and Au) with respect to the Au surface and weakening of the Thi$\cdots$Au interaction. On the other hand, the substitution of Pip^7 by D-Phe^{7}and Thi^8 by Pip^8(the [D-Arg^0,Hyp^3,Thi^5,D-Phe^7,L-Pip^8]BK analog) triggers rise of Thi^5 and Pip^8 interacts mainly through the piperidine nitrogen atom and adopts vertical orientation with respect to the Au surface. Subsequent modification (the Aaa[D-Arg^0,Hyp^3,Thi^5,D-Phe^7,L-Pip^8]BK analog) moves the Thi^5 away from the Au surface and forces tilting of the Pip^8 ring on this surface.

(iii) The Arg residue of BK and its three analogues: [D-Arg^0,Hyp^3,Thi^{5,8},L-Pip^7]BK, [D-Arg^0,Hyp^3,Thi^5,D-Phe^7,L-Pip^8]BK, and Aaa[D-Arg^0,Hyp^3,Thi^5,D-Phe^7, L-Pip^8]BK evidently participate in the adsorption process on the colloidal Au surface; the lack of Aaa SERS bands and the enhancement of the modes due to the residues from the *C*-terminal peptide end (at 5, 7, and 8 positions in the amino acid sequence) designate Arg at 9 position to be that one which interacts with the Au surface.

Conflict of Interests

The authors declare that there is no conflict of interests regarding the publication of the paper.

Acknowledgment

This work was supported by the National Research Center of the Ministry of Science and Higher Education (Grant no. N N204 544339 to Edyta Proniewicz and Grant no. 2012/05/N/ST4/00175 to Dominika Skołuba). Dominika Skołuba acknowledges the Marian Smoluchowski Krakow Scientific Consortium: "Matter-Energy-Future" (KNOW) for financial support, scholarship.

References

[1] J. M. Stewart, "Bradykinin antagonists: development and applications," *Biopolymers*, vol. 37, no. 2, pp. 143–155, 1995.

[2] D. Regoli, S. Nsa Allogho, A. Rizzi, and F. J. Gobeil, "Bradykinin receptors and their antagonists," *European Journal of Pharmacology*, vol. 348, no. 1, pp. 1–10, 1998.

[3] M. Maurer, M. Bader, M. Bas et al., "New topics in bradykinin research," *Allergy*, vol. 66, no. 11, pp. 1397–1406, 2011.

[4] J. M. Stewart, "Bradykinin antagonists as anti-cancer agents," *Current Pharmaceutical Design*, vol. 9, no. 25, pp. 2036–2042, 2003.

[5] P. A. Bunn Jr., D. Chan, D. G. Dienhart, R. Tolley, M. Tagawa, and P. B. Jewett, "Neuropeptide signal transduction in lung cancer: clinical implications of bradykinin sensitivity and overall heterogeneity," *Cancer Research*, vol. 52, no. 1, pp. 24–31, 1992.

[6] J. Enquist, C. Skröder, J. L. Whistler, and L. M. F. Leeb-Lundberg, "Kinins promote B_2 receptor endocytosis and delay constitutive B_1 receptor endocytosis," *Molecular Pharmacology*, vol. 71, no. 2, pp. 494–507, 2007.

[7] F. Horn, E. Bettler, L. Oliveira, F. Campagne, F. E. Cohen, and G. Vriend, "GPCRDB information system for G protein-coupled receptors," *Nucleic Acids Research*, vol. 31, no. 1, pp. 294–297, 2003.

[8] X. Zhang, J. L. Lowry, V. Brovkovych, and R. A. Skidgel, "Characterization of dual agonists for kinin B_1 and B_2 receptors and their biased activation of B2 receptors," *Cellular Signalling*, vol. 24, pp. 1619–1631, 2012.

[9] C. Bonechi, S. Ristori, G. Martini, S. Martini, and C. Rossi, "Study of bradykinin conformation in the presence of model membrane by nuclear magnetic resonance and molecular modelling," *Biochimica et Biophysica Acta*, vol. 1788, no. 3, pp. 708–716, 2009.

[10] J. K. Young and R. P. Hicks, "NMR and molecular modeling investigations of the neuropeptide bradykinin in three different solvent systems: DMSO, 9 : 1 dioxane/water, and in the presence of 7.4 mM lyso phosphatidylcholine micelles," *Biopolymers*, vol. 34, no. 5, pp. 611–623, 1994.

[11] D. J. Kyle, S. Chakravarty, J. A. Sinsko, and T. M. Stormann, "A proposed model of bradykinin bound to the rat B_2 receptor and its utility for drug design," *Journal of Medicinal Chemistry*, vol. 37, no. 9, pp. 1347–1354, 1994.

[12] M. Manna and C. Mukhopadhyay, "Molecular dynamics simulations of the interactions of kinin peptides with an anionic POPG bilayer," *Langmuir*, vol. 27, no. 7, pp. 3713–3722, 2011.

[13] S. C. Lee, A. F. Russell, and W. D. Laidig, "Three-dimensional structure of bradykinin in SDS micelles. Study using nuclear magnetic resonance, distance geometry, and restrained molecular mechanics and dynamics," *International Journal of Peptide and Protein Research*, vol. 35, no. 5, pp. 367–377, 1990.

[14] E. Proniewicz, D. Skoluba, I. Ignatjev et al., "Influence of applied potential on bradykinin adsorption onto Ag, Au, and Cu electrodes," *Journal of Raman Spectroscopy*, vol. 44, pp. 655–664, 2013.

[15] M. Śleszyńska, T. H. Wierzba, K. Malinowski et al., "Novel bradykinin analogues modified in the N-terminal part of the molecule with a variety of acyl substituents," *International Journal of Peptide Research and Therapeutics*, vol. 18, pp. 117–124, 2012.

[16] E. Proniewicz, I. Ignatjev, G. Niaura, D. Sobolewski, A. Prahl, and L. M. Proniewicz, "Role of Phe-D5 isotopically labeled analogues of bradykinin on elucidation of its adsorption mode on Ag, Au, and Cu electrodes. Surface-enhanced Raman spectroscopy studies," *Journal of Raman Spectroscopy*.

[17] E. Proniewicz, D. Skoluba, A. Kudelski et al., "B2 bradykinin receptor antagonists: adsorption mechanism on electrochemically roughened Ag substrate," *Journal of Raman Spectroscopy*, vol. 44, pp. 205–211, 2013.

[18] D. Sobolewski, E. Proniewicz, D. Skoluba et al., "Characterization of adsorption mode of new B2 bradykinin receptor antagonists onto colloidal Ag substrate," *Journal of Raman Spectroscopy*, vol. 44, pp. 212–218, 2013.

[19] E. Podstawka, Y. Ozaki, and L. M. Pronicwicz, "Structures and bonding on a colloidal silver surface of the various length carboxyl terminal fragments of bombesin," *Langmuir*, vol. 24, no. 19, pp. 10807–10816, 2008.

[20] E. Podstawka-Proniewicz, I. Ignatjev, G. Niaura, and L. M. Proniewicz, "Phe-MetNH2 terminal bombesin subfamily peptides: potential induced changes in adsorption on Ag, Au, and Cu electrodes monitored by SERS," *Journal of Physical Chemistry C*, vol. 116, no. 6, pp. 4189–4200, 2012.

[21] E. Podstawka-Proniewicz, D. Sobolewski, A. Prahl, Y. Kim, and L. M. Proniewicz, "Structure and conformation of Arg8 vasopressin modified analogs," *Journal of Raman Spectroscopy*, vol. 43, no. 1, pp. 51–60, 2012.

[22] E. Podstawka-Proniewicz, A. Kudelski, Y. Kim, and L. M. Proniewicz, "Structure of monolayers formed from neurotensin and its single-site mutants: vibrational spectroscopic studies," *Journal of Physical Chemistry B*, vol. 115, no. 20, pp. 6709–6721, 2011.

[23] J. Zhao, A. O. Pinchuk, J. M. McMahon et al., "Methods for describing the electromagnetic properties of silver and gold nanoparticles," *Accounts of Chemical Research*, vol. 41, no. 12, pp. 1710–1720, 2008.

[24] J. Kneipp, H. Kneipp, M. McLaughlin, D. Brown, and K. Kneipp, "In vivo molecular probing of cellular compartments with gold nanoparticles and nanoaggregates," *Nano Letters*, vol. 6, no. 10, pp. 2225–2231, 2006.

[25] C. J. Murphy, A. M. Gole, J. W. Stone et al., "Gold nanoparticles in biology: beyond toxicity to cellular imaging," *Accounts of Chemical Research*, vol. 41, no. 12, pp. 1721–1730, 2008.

[26] S.-S. Wang, "p-Alkoxybenzyl alcohol resin and p-alkoxybenzyloxycarbonylhydrazide resin for solid phase synthesis of protected peptide fragments," *Journal of the American Chemical Society*, vol. 95, no. 4, pp. 1328–1333, 1973.

[27] E. Podstawka, Y. Ozaki, and L. M. Proniewicz, "Part III: surface-enhanced raman scattering of amino acids and their homodipeptide monolayers deposited onto colloidal gold surface," *Applied Spectroscopy*, vol. 59, no. 12, pp. 1516–1526, 2005.

[28] A. E. Aliaga, C. Garrido, P. Leyton et al., "SERS and theoretical studies of arginine," *Spectrochimica Acta Part A*, vol. 76, no. 5, pp. 458–463, 2010.

[29] C. Parlak, "Theoretical and experimental vibrational spectroscopic study of 4-(1-pyrrolidinyl)piperidine," *Journal of Molecular Structure*, vol. 966, no. 1–3, pp. 1–7, 2010.

[30] Y. Hao and Y. Fang, "Piperidine adsorption on two different silver electrodes: a combined surface enhanced Raman spectroscopy and density functional theory study," *Journal of Nanoparticle Research*, vol. 9, no. 5, pp. 817–824, 2007.

[31] D. K. Singh, S. K. Srivastava, A. K. Ojha, and B. P. Asthana, "Vibrational study of thiophene and its solvation in two polar solvents, DMSO and methanol by Raman spectroscopy combined with ab initio and DFT calculations," *Journal of Molecular Structure*, vol. 892, no. 1–3, pp. 384–391, 2008.

[32] J. Yang, J. Li, and Y. Mo, "The vibrational structures of furan, pyrrole, and thiophene cations studied by zero kinetic energy photoelectron spectroscopy," *Journal of Chemical Physics*, vol. 125, no. 17, Article ID 174313, 2006.

[33] T. Matsuura and Y. Shimoyama, "Growth kinetics of self-assembled monolayers of thiophene and terthiophene on

Au(111): an infrared spectroscopic study," *European Physical Journal E*, vol. 7, no. 3, pp. 233–240, 2002.

[34] M. Moskovits, "Surface selection rules," *The Journal of Chemical Physics*, vol. 77, no. 9, pp. 4408–4416, 1982.

[35] P. Gao and M. J. Weaver, "Surface-enhanced Raman spectroscopy as a probe of adsorbate-surface bonding: benzene and monosubstituted benzenes adsorbed at gold electrodes," *Journal of Physical Chemistry*, vol. 89, no. 23, pp. 5040–5046, 1985.